Published in final edited form as:
Biomaterials. 2013 September ; 34(27): 6355–6366. doi:10.1016/j.biomaterials.2013.04.045.

PGS:Gelatin Nanofibrous Scaffolds with Tunable Mechanical and Structural Properties for Engineering Cardiac Tissues

Mahshid Kharaziha[1,2,3,*], **Mehdi Nikkhah**[1,2,*], **Su-Ryon Shin**[1,2,4], **Nasim Annabi**[1,2,4], **Nafiseh Masoumi**[1,2], **Akhilesh K. Gaharwar**[1,2,4,5], **Gulden Camci-Unal**[1,2], and **Ali Khademhosseini**[1,2,4]

[1]Center for Biomedical Engineering, Department of Medicine, Brigham and Women's Hospital, Harvard Medical School, Boston, MA, 02139, USA

[2]Harvard-MIT Division of Health Sciences and Technology, Massachusetts Institute of Technology, Cambridge, MA, 02139, USA

[3]Biomaterials Research Group, Department of Materials Engineering, Isfahan University of Technology, Isfahan, 8415683111, Iran

[4]Wyss Institute for Biologically Inspired Engineering, Harvard University, Boston, MA, 02115, USA

[5]David H. Koch Institute for Integrative Cancer Research, Massachusetts Institute of Technology, Cambridge, MA 02139, USA

Abstract

A significant challenge in cardiac tissue engineering is the development of biomimetic grafts that can potentially promote myocardial repair and regeneration. A number of approaches have used engineered scaffolds to mimic the architecture of the native myocardium tissue and precisely regulate cardiac cell functions. However previous attempts have not been able to simultaneously recapitulate chemical, mechanical, and structural properties of the myocardial extracellular matrix (ECM). In this study, we utilized an electrospinning approach to fabricate elastomeric biodegradable poly(glycerol-sebacate) (PGS):gelatin scaffolds with a wide range of chemical composition, stiffness and anisotropy. Our findings demonstrated that through incorporation of PGS, it is possible to create nanofibrous scaffolds with well-defined anisotropy that mimics the left ventricular myocardium architecture. Furthermore, we studied attachment, proliferation, differentiation and alignment of neonatal rat cardiac fibroblast cells (CFs) as well as protein expression, alignment, and contractile function of cardiomyocyte (CMs) on PGS:gelatin scaffolds with variable amount of PGS. Notably, aligned nanofibrous scaffold, consisting of 33 wt. % PGS, induced optimal synchronous contractions of CMs while significantly enhanced cellular alignment. Overall, our study suggests that the aligned nanofibrous PGS:gelatin scaffold support cardiac cell organization, phenotype and contraction and could potentially be used to develop clinically relevant constructs for cardiac tissue engineering.

CORRESPONDING AUTHOR: Ali Khademhosseini (alik@rics.bwh.harvard.edu).
*These authors equally contributed to this work.

Keywords

Scaffold; Nanofibrous; PGS:gelatin; Cardiac Cells; Tissue Engineering

1. INTRODUCTION

The extracellular matrix (ECM) of the myocardial tissue exhibits well-defined three dimensional (3D) fibrillar architecture, which provides the essential signaling cues for alignment, organization and synchronized beating of cardiac cells [1]. Collagen type I and III are the major fibrous protein components of the myocardium ECM, which play an essential role in structural integrity and mechanical robustness of the tissue construct [1, 2]. Specifically, collagen type III provides the elasticity of the matrix while collagen type I contributes to the overall rigidity of the myocardial tissue. Various combinations of these proteins result in a wide range of mechanical properties within healthy and diseased tissues [3, 4].

The synchronized beating of cardiomyocytes (CMs) and the overall contractile properties of the cardiac tissue are directly correlated to anisotropic structure of myocardial architecture [1]. To date, numerous studies have focused on simulating the anisotropic structure of myocardium thorough development of a series of biophysical cues including patterned topographical features [5–8], well-organized fibrous scaffolds [9–11] and mechanical stress [12, 13]. For example, electrospinning technique has been widely used as a simple yet versatile method in fabricating highly porous micro- and nanofibrous scaffolds comprised of interconnected pores to mimic the architecture of native myocardium. Such fibrous scaffolds could potentially induce cellular alignment and enhance migration along with cell-cell junction that ultimately result in the formation of vascularized tissue constructs [14].

In this regard, engineering of appropriate matrix compositions in terms of structural, chemical and mechanical characteristics plays a crucial role in the formation of functional cardiac tissue constructs. A suitable biomaterial could induce proper chemical and physical signaling cues that transduce into intracellular rheological and biochemical responses to modulate the cellular function [15]. So far, different types of natural and synthetic polymeric biomaterials and hydrogels have been used to generate physiologically relevant scaffolds for cardiac tissue engineering applications. For instance, gelatin, which is a mechanically robust protein, has been widely applied to develop scaffolds for cardiac grafts. Previous studies have shown that such grafts could induce spontaneous beating of CMs [16]. As gelatin degrades relatively fast [17], the use of other types of synthetic polymers such as polyglycolic acid (PGA), poly e-caprolactone (PCL), polylactic acid (PLA) and polyurethane, with slower degradation kinetics, have been investigated to fabricate cardiac grafts with slower degradation rates [10, 18–20]. However, exposure of these polymers to long-term cyclic strain, have usually resulted in plastic deformation and structural failure of the construct. Therefore, in order to overcome these limitations, it is beneficial to develop an elastomeric biomaterial with appropriate mechanical, chemical and degradation properties.

Poly(glycerol-sebacate) (PGS) is a non-cytotoxic and biodegradable elastomer (stiffness ~ 0.056–1.5 MPa) [21], which has been widely used in several tissue engineering applications such as nerve, heart and vascular systems [22–24]. For example, PGS has been previously used to develop microfabricated anisotropic accordion-like honeycomb microstructure [25] to support synchronized beating of the cardiac cells. Alternatively, other studies have explored the use of poly(3-hydroxybutyrate-co-3-hydroxyvalerate):PGS microfibrous scaffolds [26] and PGS:PLA [27] and core-shell PGS:gelatin [28] fibrous structures for cardiac tissue engineering applications. However, the majority of the above mentioned

scaffolds were associated with significant limitations such as complex fabrication process, inability to precisely control the properties of the scaffolds, formation of random fibrous structures, limited fiber size (microscale range) and high degradation rate [26–28]. For example, core-shell fibrous scaffolds usually consist of large fiber size (in the range of 1–1.5 μm) where the core material dictates the mechanical properties of the fiber, and the shell polymer solely affects the cell functions. In addition, the fabrication technique of these types of scaffolds does not easily allow modulation of the desired ratio between the two polymers [27, 28]. Therefore, it is envisioned that through blending an elastomeric polymer (i.e. PGS) with a fairly rigid biomaterial (i.e. crosslinked gelatin), it would be possible to develop a family of biomaterials with a wide range of architectural, chemical and mechanical properties as suitable microenvironments for 3D culture and maturation of cardiac cells (i.e. cardiac fibroblasts (CFs) and CMs).

In this paper, we developed elastomeric PGS:gelatin nanofibrous scaffolds for engineering of the myocardium tissue. In particular, we fabricated and characterized elastomeric nanofibrous PGS:gelatin scaffolds with a wide range of compositions through blending of PGS and gelatin for engineering of the myocardium tissue. We hypothesized that enhanced function of the engineered myocardium tissue significantly relies on the coupled chemical and physical characteristics of the polymeric matrix. Furthermore, we extensively studied cardiac cell behavior including alignment, attachment, proliferation, protein expression, maturation and contraction on the developed PGS:gelatin scaffolds.

2. MATERIALS AND METHODS

2.1. Fabrication and crosslinking of fibrous PGS:Gelatin scaffolds

PGS:gelatin fibrous scaffolds with variable compositions were prepared using electrospinning techniques. Primarily, PGS prepolymer (M_W=10,000) was synthesized according to the previously reported procedures [29]. Briefly, a stoichiometric amount of sebacic acid and glycerol with 1:1 molar ratio was reacted at 120°C under nitrogen and high vacuum (less than 50 mTorr) for 24 h to synthesize PGS prepolymer [29]. In order to define an optimum scaffold for myocardial regeneration, we varied the amount of PGS and gelatin within the scaffold at different weight ratios (2:1, 1:2 and 0:1) in 80% (v/v) acetic acid solution and mixed at a final polymer concentration of 20% (w/v). For the electrospinning process, a syringe pump was used to inject the polymer solution into a 1 mL syringe having a 23G blunted stainless steel needle. The flow rate was set to 2 mL/h. The distance in between the collector and needle was set to 10 cm while the voltage was kept at 18 kV constant during the electrospinning process. In order to fabricate aligned scaffolds, parallel electrodes made of aluminum foil were used as collectors while for the random fibers a glass slide was placed on the collector plate. Aligned and random scaffolds were named as A(2PGS:Gelatin), A(PGS:2Gelatin) , A(Gelatin) as well as R(2PGS:Gelatin), R(PGS: 2Gelatin) , R(Gelatin) respectively where letters A and R defines the type of scaffold and 2:1, 1:2 and 0:1 corresponds to 66%, 33% and 0 wt.% PGS content. The fabricated scaffolds were dried overnight under vacuum prior to further characterizations and biological experiments.

For crosslinking process, the electrospun scaffolds were immersed in 90% (v/v) ethanol solution containing N,N-(3-dimethylaminopropyl)-N'-ethyl-carbodiimide hydrochloride (EDC) and N-hydroxysuccinimide (NHS) for 12 h at 4 °C. EDC concentration was optimized at 75 mM and the molar ratio of EDC/NHS was selected to be 2.5:1 for crosslinking of gelatin. The scaffolds were then washed with Dulbecco’s phosphate buffered saline (DPBS, Gibco, USA) three times to remove the residual of crosslinking agent.

2.2 Characterization of nanofibrous scaffold

The surface topographies of the electrospun scaffolds, before and after crosslinking process, were characterized using scanning electron microscopy (SEM) analysis using a FEI/Philips XL30 FEG SEM (15 kV). Samples were sputter-coated with a thin layer of gold/palladium and the SEM images along with NIH Image J software were used to measure the fiber and pore sizes (n=50) of the scaffolds. Fourier-transform infrared spectroscopy (FTIR) (Bruker Optics, MA, USA) was performed over a range of 500–4000 cm^{-1} and resolution of 2 cm^{-1} to verify the chemical composition of the scaffolds. Hydrophilic properties of the developed PGS:gelatin scaffolds (n=3) were determined by water contact angle measurement using the static sessile drop technique. The contact angle of the scaffolds was measured using video contact angle measurement setup (VCA Optima, AST Inc.). The average of the measured values (n=3) were reported with standard deviation.

The mechanical properties of the PGS:gelatin scaffolds were determined by using uniaxial tensile testing technique (Instron, Model 5542) with 10 N load capacity at a rate of 7 mm/min. Samples were prepared in rectangular-shape pieces with a length of 4–5 mm, width of 6–8 mm and thickness of 0.3–0.5 mm. At least 5 samples were prepared for each scaffold composition. The tensile properties were measured before and after crosslinking, in dry and wet conditions. For wet condition, scaffolds were soaked in culture medium (Dulbecco's modified eagle medium (DMEM, Gibco, USA)) for 2 days at 37 °C prior to experimental testing. Tensile strength, Young's modulus (stiffness), and strain at break (elongation) were determined from the stress–strain curves. Stiffness was measured from the slope of the linear segment of the stress–strain graph (5–10%), while elongation was obtained when samples failed. Measured values were reported as mean standard deviation (SD).

In vitro degradation assay was used to study the weight loss of the scaffolds (n=3) with dimensions of 5 mm × 5 mm × 0.5 mm (length, width, thickness). The samples were incubated in DPBS at 37 °C for 1, 4, 7, 14, 21 and 28 days. DPBS was changed every 3 days. After each specific time point, the scaffolds were rinsed in DPBS, weighed and lyophilized using a freeze-dryer for overnight. The weight of dried samples was determined after lyphilization. The percent degradation for each sample was calculated by dividing the weight loss to the initial dry weight.

2.3. Cell culture

2.3.1. Isolation and culture of rat CMs and CFs—Fibrous scaffolds on glass slides were placed in a 24-well plate and sterilized for 30 min in 70% (v/v) ethanol and overnight under UV light. The scaffolds were then immersed in cardiac medium consisting of DMEM containing 10 % (v/v) fetal bovine serum (FBS, Gibco, USA), 1% (v/v) L-Glutamine (Gibco, USA) and 100 units/ml penicillin-streptomycin (Gibco, USA) for overnight prior to cell seeding. Neonatal rat ventricular CMs and CFs were isolated from 2-day-old Sprague-Dawley rats according to a well-established protocol approved by the Institute's Committee on Animal Care [30]. CMs were used after their isolation and enrichment through 1 h pre-plating. They were collected from the flask, counted and seeded on the samples (n=3) with a density of 1.4×10^6 cells/cm^2. In addition, CFs (passage 1) were trypsinized and seeded on the separate set of scaffolds (n = 6) and tissue culture plate (TCP) and PGS films, as control, with a density of 0.3×10^5 cells/cm^2.

2.3.2. CFs attachment viability, and metabolic activity—The CFs attachment on the scaffolds was determined by using DNA quantification assay (Quant-iT™ PicoGreen®, Invitrogen, USA), according to the manufacturer's protocol. Scaffolds (n=3) were rinsed with DPBS and weighed at wet condition. The samples were then digested overnight at 60°C in 1 mL of DNA extraction solution. To prepare DNA extracted solution, PBE buffer

was prepared by dissolving Na_2HPO_4 (14.2 mg/ml) and EDTA (2.3 mg/ml) (Sigma-Aldrich) in deionized water and adjusting the pH to 6.5 using 1M HCl solution. Then, L-cystein (1.6 mg/ml) was added to 20 ml of DNA extracted solution and the prepared solution was mixed with papain (0.5%(v/v)). Finally, 1X PicoGreen solution (50% (v/v)) was added to digested sample solution (50% (v/v)) and their absorbance were measured at 485 nm wavelength.

CFs viability was determined after 1, 3, and 5 days of culture, using calcein-AM/ethidium homodimer Live/Dead assay (Invitrogen). Scaffolds were rinsed with DPBS and the live/dead solution was added to each sample and placed inside incubator for 20 min. The samples were then imaged using an inverted fluorescence microscope (Nikon TE 2000-U, Nikon instruments Inc., USA). The cell viability was determined using Image J software by the number of live cells (green stain) divided by total cell number (green and red stain).

CFs metabolic activity on the scaffolds was determined by using the Alamar Blue (AB) assay (Invitrogen) at days 0 (6 h), 3 and 5 of culture on fibrous scaffolds and TCP and PGS films as control condition. Briefly, 400 μl of AB solution dissolved in warm culture medium (10% (v/v)) was added to each well and placed inside incubator for 3 h. Then, 100 μl of the reduced-color culture medium within each well was transferred to 96-well plate in duplicate and absorbance was measured at 544–590 nm wavelength. Finally, the normalized metabolic activity with respect to day 0 was calculated for each scaffold.

2.3.3 Immunostaining for cell cytoskeletal organization, α-smooth muscle actin (α-SMA) and CMs marker expression—Immunostaining was performed to assess the cytoskeletal organization (F-actin) of CFs at days 1, 3 and 5 of culture. The samples were fixed in 4% (v/v) paraformaldehyde (PF) solution in DPBS for 20 min at room temperature, permeabilized in 0.1% (v/v) Triton X-100 in DPBS for 30 min and then blocked in 1% (v/v) Bovine Serum albumin (BSA) for 1 h. The cells were then stained for F-actin using 1:400 dilution of Alexa Fluor-594 phalloidin (Invitrogen) in 1% (v/v) BSA. α-SMA marker was used to identify the differentiation of CFs to myofibroblast phenotype at day 1 and 5 of culture. Upon fixation, the samples were permeabilized in methanol for 10 min. Primary antibody (Sigma) was added to each well and the samples were incubated for 1 h at room temperature. The samples were then washed in DPBS for three times, and a 1:200 dilution of the Alexa Fluor-598 conjugated anti-rabbit was added. In order to quantify the number of the differentiated cells within each scaffold and control substrates (TCP), they were co-stained by (α-SMA)/(F-actin) (3 sample for each condition, 3 random images for each samples) and the projected areas of their signals were calculated using image J software. The α-SMA–positive cell numbers were normalized to the F-actin signals [31].

Immunostaining for CMs markers was performed using three different cardiac-specific proteins including sarcomeric α-actinin, connexin-43 (Cx-43), and troponin I after 7 days of culture. After fixation and permeabilization, the cell-seeded scaffolds were blocked in 10% (v/v) goat serum (GS). A 1:200 dilution of primary antibodies specific to sarcomeric α-actinin, Cx-43 and troponin I in 10% (v/v) GS was then added to the samples and they were kept at 4 °C for 24 h. The scaffolds were then washed three times in DPBS and a 1:200 dilution of Alexa Fluor-488 conjugated goat anti-mouse secondary antibody for sarcomeric α-actinin, Alexa Fluor-594 goat anti-mouse secondary antibody for troponin, and Alexa Fluor-594 goat anti-rabbit secondary antibody for Cx-43 were added to samples. The scaffolds were kept in dark for 40 min at room temperature. Following immunostaining, the cells' nuclei were stained with 1:1000 dilution of 4′,6-diamidino-2-phenyl indole dihydrochloride (DAPI) stain (Invitrogen) in DPBS for 5 min. The samples were visualized using a fluorescence microscope (Nikon TE 2000-U, Nikon instruments Inc., USA) and the images were analyzed using image J software.

2.3.4 Collagen assay—The amount of newly synthesized and deposited collagen produced during CFs culture on the scaffolds was estimated using collagen assay. After removing the culture medium, samples were rinsed three times in DPBS, weighed, cut, and digested with 500 mL of pepsin solution (0.25mg/mL). Collagen assay was preformed according to the picrosirius red-based colorimetric assay (SirCol™ collagen dye binding assay kit, Biocolor Ltd.). Collagen concentration was obtained from absorbance measured at 540 nm and standard curve prepared according to the protocol. The absorbance of water was also recorded as blanked. In addition, pure crosslinked gelatin scaffold was prepared and collagen assay was preformed on it to remove the effects of gelatin on the collagen absorbance.

2.3.5. Characterization of beating behavior of cardiomyocytes—The beating behavior of CMs was measured every day using a real-time imaging and video recording system and a custom written MATLAB program starting from day 3 of culture to assess CMs electrophysiological property [32]. The beating rates of CMs on scaffolds were counted at three different points.

2.3.6 Quantification of cellular alignment—After 1, 3 and 5 days of culture, the scaffolds were fixed in 4% PFA and DAPI was used to stain the cells' nuclei to quantify cellular alignment within aligned and random scaffolds. Fluorescence images were obtained at 5–6 different locations of each sample (Cell number=800–1600). The shape of each nuclei was primarily fitted with an ellipse, then the cells nuclei alignment angles within each image were calculated using Image J software. Finally, The overall nuclear alignment was normalized to the average nuclear alignment within each fluorescence image. The histograms of normalized alignment angles were defined to compare the nuclei alignment within each condition. Similar to estimation of alignment, cell elongation was also evaluated using fluorescence F-actin images from 5–6 regions of each sample and analyzed by image J software. Cell elongation was determined as the aspect ratio between the cell length and cell breadth (cell length/cell breath). The longest cord within the cell body was selected as the cell length while the cell breadth defined as the shortest cord perpendicular to the length.

2.4. Statistical Analysis

All data were presented in mean ± standard deviation (SD) and statistical significance was measured by performing one-way ANOVA analysis followed by Tukey's multiple comparison using GraphPad, Prism Software (V.5). Differences were taken to be significant for $P < 0.05$.

3. RESULTS AND DISCUSSION

3.1. Development and characterization of nanofibrous scaffolds

The structural matrix of myocardial ECM consists of nano-fibrillar collagen types I and III, which provides proper physical and chemical to modulate cardiac function [33]. The main objective of this study was to fabricate PGS:gelatin nanofibrous scaffolds using electrospinning technique to create an optimized matrix to mimic the native myocardial tissues and study CMs and CFs behavior.

Using electrospinning technique, nanoscale fibers could be organized into various architectures depending upon the collector type (Supplementary Fig. S1(A)). Since gelatin is water soluble, crosslinking was required to stabilize its structure. Electrospun PGS:gelatin scaffolds were crosslinked by using EDC/NHS, which is less cytotoxic compared to other crosslinker such as glutaraldehyde [34]. SEM images (Fig. 1(A)) clearly demonstrated that crosslinking process resulted in larger fibers that were curled and fused together at multiple

junctions. Specifically, the fiber size within aligned pure gelatin scaffolds increased 2-folds from 250±28 nm to 520±35 nm which might be due to swelling of the fibers during the crosslinking process. Similar to its uncrosslinked state, the fiber size and pore size significantly ($P<0.05$) decreased while the number of junctions increased as a function of PGS content (Fig.1(B)). Specifically, the pore sizes of random fibrous scaffolds decreased from 10.4±1.6 μm within R(Gelatin) scaffold to 7.7 ±3.0 μm on R(2PGS:Gelatin) scaffolds. Within the aligned fibrous scaffolds, the pore size decreased by 2-folds from A(Gelatin) to A(2PGS:Gelatin) scaffold (Fig.1(C)).

Chemical characterization of scaffolds as well as PGS film (control) was conducted using FTIR analysis (Fig.1(D) and Supplementary Fig. S1(B)). Crosslinking process of gelatin within all the scaffolds was confirmed through shifting of the characteristic bands of gelatin peptide chain (i.e. amide I, amide II and amide III) to lower wavenumbers along with reduced intensity ratio of $A_{\text{amid I}}/A_{\text{amid II}}$. These factors are mainly due to the reaction of carboxyl groups of amino acids originated from aspartic acid as well as the formation of new covalent C-N bond [34]. Furthermore, the lower intensity ratios of –COOH and –OH groups of PGS within the crosslinked blended scaffolds compared to pure PGS prepolymer film ($A_{[-COOH]}/A_{[-OH]}$) indicated the formation of carbonyl (C=O) groups and involvement of PGS during the crosslinking process. Furthermore, the sebacic acid bands of PGS at 930 cm^{-1} and 1300 cm^{-1} disappeared and the intensity of carbonyl (C=O) band shifted to a lower wavenumber confirming that PGS polymer was involved in the crosslinking process [35, 36].

The *in vitro* degradation of the scaffolds was monitored over a month period (Fig. 1(E)). Degradation of the scaffolds was determined to be changing as a function of topographical cues as well as the chemical composition of the scaffolds. The weight loss of all scaffolds demonstrated an approximate linear profile while the blended scaffolds exhibited lower weight loss compared to pure gelatin scaffold. The degradation profile of pure gelatin scaffolds is expected to be due to the hydrolysis of the carboxyl-amino groups. Alternatively, within the blended scaffolds decomposition of ester bonds of PGS into its sebacic acid and glycerol monomers dictates the degradation rate of the scaffolds. Therefore, higher number of ester bonds induced longer degradation times [36]. In addition to chemical factors, topographical cues such as pore size and alignment of the fibers are expected to affect the degradation profile of the scaffolds. The larger pore size of pure gelatin scaffold likely accelerated the hydrolysis and the weight loss of the scaffold compared to their blended analogs due to the increased contact area and permeability of the scaffolds with DPBS.

Since extremely stiff substrates inhibit the contractile properties of cardiac cells, relatively elastic scaffolds (similar to native tissue tensile modulus ~ 54–240 kPa) could potentially provide a suitable microenvironment to mimic the native myocardial tissue [9, 37, 38]. Detailed mechanical properties of the scaffolds after and before crosslinking are listed in Table 1 and Supplementary Fig. S2(A–C) respectively. Crosslinking process improved the overall mechanical properties of scaffolds due to inter- and intra-molecular covalent bonds and the formation of point-point junctions between the fibers. The presence of these bonds reduced the extensibility of the fiber but increased stiffness and strength similar to the other reports in the literature [39, 40].

Fig. 1(F) shows the representative stress–strain curves of the crosslinked aligned and random (Gelatin) and (2PGS:Gelatin) scaffolds after 2 days in culture medium. All scaffolds exhibited similar strain-stress trends; a linear region followed by non-linear region without the necking phenomenon. Overall, in hydrated condition, the scaffolds exhibit low stiffness and high elongation compared to the dry state. This might be due to the presence of hydrated

and highly entangled polymer chains, which facilitate chain sliding under mechanical deformation [41]. On the other hand, addition of PGS significantly ($P<0.05$) decreased stiffness and enhanced elongation in both dry and wet states. This is mainly attributed to the plasticizing effects of PGS on the mechanical properties of the blended scaffolds.

In addition to chemical composition, the architecture of the scaffolds also influenced their mechanical properties; within both dry and wet states, aligned fibrous scaffolds exhibited notably higher stiffness and strength compared to the random ones, while elongation remained unaltered (Table I). This is expected mainly because of the orientation of the fibers along with the direction of the tensile load [41, 42]. Furthermore, according to previous results, the increased fiber size within random scaffolds reduced their strength and stiffness since the scaffolds displayed bulk-like properties making the stretching of the polymer chains more difficult [41, 43].

In general, material and structural characterization of the blended construct indicated that incorporation of PGS within the nanofibrous scaffold significantly reduced the overall stiffness of the matrix at wet condition, mimicking the elasticity of myocardium [25].

3.2. CFs culture on PGS: gelatin scaffolds

To assess the behavior of cells on PGS: gelatin scaffolds, we primarily analyzed viability of the CFs that were seeded on the developed scaffolds. Representative live/dead fluorescence and phase contrast image (Fig. 2(A)), demonstrated high cellular viability (>90%), alignment and fillapodia extension along the direction of the fibers (Fig. 2(B)). DNA quantification demonstrated that increasing PGS content significantly ($P<0.05$) enhanced cell attachment on both aligned and random scaffolds (Fig. 2(C)). Although all scaffolds were hydrophilic, A(Gelatin) scaffold had lower contact angle compared to A(PGS: 2Gelatin) and A(2PGS:Gelatin) scaffolds (Supplementary Fig. S2(D)). On the other hand, it is well known that cell adhesion is stronger on stiff substrates compared to the compliant (soft) ones [44]. Therefore, higher cell attachment on the scaffolds with higher PGS content (softer substrate) is expected to be mainly dominated by the smaller fiber size, higher surface-to-volume ratio, which ultimately enhances protein adsorption as well as selective protein secretions as a favorable substrate for cell attachment [45]. Similar observations were reported for other polymers such as PLGA/collagen [46], Poly(L-lactide-co-3-caprolactone)(PLCL)/gelatin [47] and PLCL/collagen [48] fibrous scaffolds where a lower concentration of natural polymers resulted in increased cellular adhesion. CFs exhibited significantly enhanced metabolic activity on the fibrous scaffolds compared to pure PGS films (control) (Fig. 2(D)). In addition, decreasing PGS content along with the architecture of the scaffold (Aligned vs. Random) significantly ($P<0.05$) promoted proliferation of the cells (at day 5) suggesting that CFs metabolic activity was a function coupled chemical and mechanical as well as architectural properties of the scaffolds.

In the native heart tissue, the interactions between CMs and other cells such as CFs through autocrine and paracrine signaling pathways influence the function of CMs [49]. Therefore, maintaining the balance of both cell types is important to ensure proper physiological properties of the engineered tissue constructs. Furthermore, myofibroblasts, which are differentiated phenotype of fibroblastic cells, usually express high levels of ECM proteins (Collagen type I) and proliferate more than fibroblast cells [50]. Therefore, in this study, we also quantified α-SMA expression, which is a myofibroblast specific marker, along with actin cytoskeletal organization to assess the CFs differentiation on the developed scaffolds (Fig. 3(A and B)). In general, cells cultured on TCP dishes expressed more α-SMA compared to scaffolds on days 1 and 5 of culture. Furthermore, on the entire scaffolds, α-SMA expression (yellow stained cells) enhanced with decreasing PGS content. For example, α-SMA expression increased from 15% ± 6% on R(2PGS:Gelatin) to 42% ± 5% on

R(Gelatin) scaffolds after day 1 of culture (Fig. 3(A,B)). To further validate these observations, the amount of newly deposited collagen by CFs on the scaffolds was measured (Fig. 3(C)). Insoluble collagen assay showed significantly higher ($P<0.05$) amount of collagen deposition on A(Gelatin) fibrous scaffolds (20.43±13.1) compared to A(2PGS:Gelatin) scaffolds (8.9±2.1). Pure gelatin scaffolds (without cells) were used as a control condition. As expected, no collagen pellet was precipitated within pure gelatin samples during the quantification confirming the enhanced collagen expression on cell seeded-scaffolds is mainly due to the new ECM secretion. It is well respected that in addition to various hormones, cytokines and growth factors [51–53], substrate topography and mechanical properties such as stiffness [31, 54, 55] as well as culture conditions (*i.e.* medium composition, cell density and passage number) [56] also induce CFs organization, proliferation and differentiation to myofibroblasts. For example, it has been shown that silicone topographies with 10-μm vertical projections decreased CFs proliferation compared to flat membranes [57]. Furthermore, fibroblasts grown in 3D collagen gels expressed high levels of α-SMA in response to matrix stiffness and external mechanical stretch [58]. Therefore, we anticipate that higher level of α-SMA expression along with collagen deposition on pure gelatin scaffolds compared to the blended ones, specifically 2PGS:Gelatin, is mainly due to fairly higher stiffness of the matrix. In addition, we expect that higher proliferation rate of on rigid scaffolds (Gelatin) is mainly due to the differentiated state of the cells to myofibroblasts [50].

We also evaluated actin cytoskeletal organization and morphology of CFs on the fabricated scaffolds at different culture times. Actin filament staining demonstrated that the morphology and the cytoskeletal organization of the cells was significantly affected by the structural properties of the scaffolds (Fig. 4(A)). At day 1 of culture, majority of the cells exhibited spindle-shape morphology on both random and aligned scaffolds. On the random scaffolds, after 5 days of culture, cells randomly oriented and exhibited larger sizes compared to day 1 with more stress fibers. On the other hand, within the aligned scaffolds, the cells were able to sense the anisotropic topography of the underlying scaffold and aligned along the fibers direction as early as one day of culture. In general, within aligned scaffolds, stress fibers were thicker and denser than the random ones. These scaffolds also induced different degrees of cell alignment; on A(PGS:2Gleatin) scaffold, the cells were highly orientated along the fiber (~82 %) within 0–20 degree preferred angle which was significantly higher that of pure gelatin scaffolds (~ 60 %)(Fig. 4(B) and Supplementary Fig. S3). Furthermore, the effects of scaffold topography on CFs elongation were also studied through determination of cell aspect ratio (Fig. 4(C)). CFs exhibited elongated morphology and mainly migrated along the direction of the fibers. As expected, there was not a significant difference between cell elongations on the random scaffolds. However, the elongation value on A(PGS:2Gleatin) scaffold was 3-folds higher than that of the pure gelatin and 2-folds higher than A(2PGS:Geltain) scaffold respectively ($P<0.05$). One of the properties of myofibroblasts is the presence of parallel and highly organized stress fiber throughout the cytoplasm [57]. According to Fig. 3 and 4, more stress fibers were observed in α-SMA–positive CFs. These stress fibers appeared to be thicker and denser on scaffold with lower PGS content. Similarly, according to mechanical characterization of the scaffolds (Table 1), increasing PGS content resulted in higher elasticity of the matrix and lower resistance to deformation therefore leading to the formation of thinner stress fibers within cytoskeleton of CFs. These observations were consistent with the previous work of others on substrates with different ranges of stiffness [54, 55].

Previous studies have demonstrated that the majority of cell types respond to the topographical features of the underlying substrate and align along the direction of the patterns [6, 59] or fibers of scaffold [9, 60]. In addition, induction of cyclic mechanical strain results in enhanced cellular alignment [31]. Our findings were consistent with

previous reports confirming that the architecture of the fibrous scaffolds (Aligned vs. Random) significantly affect cellular alignment. Furthermore, our results indicated that the interplay between mechanical properties of the substrates (stiffness) along with chemical composition (PGS content) affected the overall cellular alignment. For instance, although chemical composition of A(2PGS:Gelatin) scaffold promoted cellular attachment compared to A(PGS:2Gelatin) scaffolds (Fig.2(C)), the cell did not exhibit improved cellular alignment. Therefore, A(PGS:2Gelatin) scaffolds provided an optimal matrix in terms of coupled chemical and mechanical properties for cellular alignment.

3.3. CMs culture on PGS:gelatin scaffolds

The ventricle myocardium posses a highly aligned and organized architecture along with contractile ability as the result of CMs coupling with their neighboring cells [61]. To further validate the suitability of the fabricated scaffolds for cardiac tissue engineering, we tested the functional and biological behavior of the CMs on the developed scaffolds. To obtain high contractility, it is necessary to confirm that CMs express homogeneously-distributed sarcomeric α-actinins [10]. Our findings demonstrated that CMs on the aligned scaffolds exhibited organized and aligned sarcomeric α-actinin in comparison to random scaffolds suggesting that sarcomeric organization was a function of scaffold topography (Fig. 5). Furthermore, CMs cultured on blended scaffolds exhibited well-defined sarcomeres compared to the ones seeded on pure gelatin scaffolds. Similarly, Cx-43, which is one of the main gap junction proteins of the CMs indicating cell-cell communication [62], was well expressed on blended scaffolds compared to A(Gelatin) and R(Gelatin) scaffolds. Cx-43 expression was found to be distributed within the cells cytoskeleton and was not limited to intercalated disks at end-to-end contacts on the random scaffolds. However, on the aligned scaffolds, cells were oriented and formed side-to-side contacts while Cx-43 were expressed in a parallel fashion within intra-cellular contact points. Since, synchronized beating of CMs is directly coupled to the expression of gap junctions [62], immunostaining results confirmed the suitability of the aligned blended scaffolds to induce synchronized beating of the cells. Notably, troponin I, which is a calcium receptive component associated with cytoskeletal organization and maturation of CMs [60], was visible along with sarcomeres on the aligned scaffolds. In contrast, the sarcomeres in CMs grown on random gelatin scaffolds appeared to be randomly distributed and immature.

Similar to CFs, CMs exhibited significantly higher alignment and organization on A(PGS:2Gelatin) scaffold compared to other scaffolds due to optimal chemical and mechanical properties of the matrix (Fig. 6(A)). Furthermore, CMs seeded on the aligned and random blended scaffolds started beating after 2 days of culture. However, the beating pattern frequency (beats per min, BPM) were significantly enhanced on the aligned scaffolds compared to the random ones (Fig. 6(B,C), Supplementary Video S1, S2). In particular, after 7 days culture, CMs on A(PGS:2Gelatin) scaffolds exhibited the highest beating rate (>60 BPM) coupled with significant alignment and organization (Fig. 6(B,C), Supplementary Video S1(b)), followed by A(2PGS:Gelatin), and finally A(Gelatin) scaffolds. Enhanced CMs beating on the A(PGS:2Gelatin) scaffolds suggested that contraction ability of CMs was affected by the scaffold architecture along with chemical and mechanical properties of the matrix.

Our study demonstrated that the CMs contraction is significantly dependent on the chemical and physical properties of the underlying substrates. When CMs are cultured on a rigid substrate mimicking a post-infarct fibrotic scar (opposed to healthy myocardium), they lose their synchronized beating. On the other hand, softer scaffolds such as A (PGS:2Gelatin) and A(2PGS:Gelatin), which mimic the elasticity of the native myocardial tissue, are suitable to induce synchronized beating [4]. Therefore, an elastomeric scaffold consisting of

optimized chemical and mechanical properties (A(PGS:2Gelatin)), can be used as suitable biomaterials for engineering functional myocardial tissue.

4. CONCLUSION

In this study, we developed aligned and random nanofibrous PGS:gelatin blended scaffolds with stiffness in the range of 140–590 kPa (R(2PGS:Gelatin)-A(PGS:2Gelatin)). We demonstrated that scaffold structure, composition and stiffness are crucial factors in directing the CFs and CMs behavior. Cellular attachment, proliferation and differentiation of CFs were mainly affected by the chemical composition and stiffness of the scaffold. The alignment and organization of the cells, were influenced by structural cues (aligned vs. random) along with stiffness of the scaffolds. Furthermore, CMs contraction, organization and maturation were affected by scaffold structure, composition and stiffness. CMs on the aligned scaffolds expressed anisotropically organized sarcomeric structures while the presence of PGS within blended scaffold improved the overall sarcomere formation on both aligned and random architectures compared to pure gelatin scaffolds. A(PGS:2Gelatin) scaffolds induced significantly higher level of cellar alignment coupled with synchronize beating compared to other scaffolds. In summary, our findings indicated that nanofibrous PGS:gelatin blended scaffolds can be used as potentially suitable constructs for myocardial regeneration and repair.

Supplementary Material

Refer to Web version on PubMed Central for supplementary material.

Acknowledgments

The authors acknowledge funding from the Presidential Early Career Award for Scientists and Engineers (PECASE), the Office of Naval Research Young National Investigator Award, the National Science Foundation CAREER Award (DMR 0847287), and the National Institutes of Health (HL092836, AR057837, DE021468, DE019024, EB012597, HL099073, EB008392) and MIT- Portugal Program (MPP-09Call-Langer-

REFERENCES

1. Tandon V, Zhang B, Radisic M, Murthy SK. Generation of tissue constructs for cardiovascular regenerative medicine: from cell procurement to scaffold design. Biotechnol Adv. 2012 In Press.
2. Brown RD, Ambler SK, Mitchell MD, Long CS. The cardiac fibroblast: therapeutic target in myocardial remodeling and failure. Annu Rev Pharmacol Toxicol. 2005:657–687. [PubMed: 15822192]
3. Marsano A, Maidhof R, Wan LQ, Wang Y, Gao J, Tandon N, et al. Scaffold stiffness affects the contractile function of three-dimensional engineered cardiac constructs. Biotechnol Prog. 2010; 26:1382–1390. [PubMed: 20945492]
4. Engler AJ, Carag-Krieger C, Johnson CP, Raab M, Tang H-Y, Speicher DW, et al. Embryonic cardiomyocytes beat best on a matrix with heart-like elasticity: scar-like rigidity inhibits beating. J Cell Sci. 2008; 121:3794–3802. [PubMed: 18957515]
5. Au HTH, Cheng I, Chowdhury MF, Radisic M. Interactive effects of surface topography and pulsatile electrical field stimulation on orientation and elongation of fibroblasts and cardiomyocytes. Biomaterials. 2007; 28:4277–4293. [PubMed: 17604100]
6. Nikkhah M, Edalat F, Manoucheri S, Khademhosseini A. Engineering microscale topographies to control the cell-substrate interface. Biomaterials. 2012; 33:5230–5246. [PubMed: 22521491]
7. Wang P-Y, Yu J, Lin J-H, Tsai W-B. Modulation of alignment, elongation and contraction of cardiomyocytes through a combination of nanotopography and rigidity of substrates. Acta Biomater. 2011; 7:3285–3293. [PubMed: 21664306]

8. Camelliti P, Gallagher JO, Kohl P, McCulloch AD. Micropatterned cell cultures on elastic membranes as an in vitro model of myocardium. Nat Protoc. 2006; 1:1379–1391. [PubMed: 17406425]
9. Kai D, Prabhakaran MP, Jin G, Ramakrishna S. Guided orientation of cardiomyocytes on electrospun aligned nanofibers for cardiac tissue engineering. J Biomed Mater Res B Appl Biomater. 2011; 98B:379–386. [PubMed: 21681953]
10. Rockwood DN, Akins RE Jr, Parrag IC, Woodhouse KA, Rabolt JF. Culture on electrospun polyurethane scaffolds decreases atrial natriuretic peptide expression by cardiomyocytes in vitro. Biomaterials. 2008; 29:4783–4791. [PubMed: 18823659]
11. Riboldi SA, Sadr N, Pigini L, Neuenschwander P, Simonet M, Mognol P, et al. Skeletal myogenesis on highly orientated microfibrous polyesterurethane scaffolds. J Biomed Mater Res A. 2008; 84A:1094–1101. [PubMed: 17685407]
12. Carrier RL, Rupnick M, Langer R, Schoen FJ, Freed LE, Vunjak-Novakovic G. Perfusion improves tissue architecture of engineered cardiac muscle. Tissue Eng. 2002; 8:175–188. [PubMed: 12031108]
13. Vandenburgh HH, Solerssi R, Shansky J, Adams JW, Henderson SA. Mechanical stimulation of organogenic cardiomyocyte growth in vitro. Am J Physiol Cell Physiol. 1996; 270:C1284–C1292.
14. Kim HN, Jiao A, Hwang NS, Kim MS, Kang DH, Kim DH, et al. Nanotopography-guided tissue engineering and regenerative medicine. Adv Drug Delivery Rev. 2012 In Press.
15. Chowdhury F, Na S, Li D, Poh Y-C, Tanaka TS, Wang F, et al. Material properties of the cell dictate stress-induced spreading and differentiation in embryonic stem cells. Nat Mater. 2010; 9:82–88. [PubMed: 19838182]
16. Li RK, Jia ZQ, Weisel RD, Mickle DAG, Choi A, Yau TM. Survival and function of bioengineered cardiac grafts. Circulation. 1999; 100:63–69.
17. Akhyari P, Fedak PWM, Weisel RD, Lee TYJ, Verma S, Mickle DAG, et al. Mechanical stretch regimen enhances the formation of bioengineered autologous cardiac muscle grafts. Circulation. 2002; 106:I137–I142. [PubMed: 12354723]
18. Shin M, Ishii O, Sueda T, Vacanti JP. Contractile cardiac grafts using a novel nanofibrous mesh. Biomaterials. 2004; 25:3717–3723. [PubMed: 15020147]
19. Mukherjee S, Gualandi C, Focarete ML, Ravichandran R, Venugopal JR, Raghunath M, et al. Elastomeric electrospun scaffolds of poly(l-lactide-co-trimethylene carbonate) for myocardial tissue engineering. J Mater Sci Mater Med. 2011; 22:1689–1699. [PubMed: 21617996]
20. Mukherjee S, Venugopal JR, Ravichandran R, Ramakrishna S, Raghunath M. Evaluation of the biocompatibility of PLACL/collagen nanostructured matrices with cardiomyocytes as a model for the regeneration of infarcted myocardium. Adv Funct Mater. 2011; 21:2291–2300.
21. Chena O, Liang S, Thouas GA. Elastomeric biomaterials for tissue engineering. Prog Polym Sci. 2013; 38:584–671.
22. Wang YD, Ameer GA, Sheppard BJ, Langer R. A tough biodegradable elastomer. Nat Biotechnol. 2002; 20:602–606. [PubMed: 12042865]
23. Sundback CA, Shyu JY, Wang YD, Faquin WC, Langer RS, Vacanti JP, et al. Biocompatibility analysis of poly(glycerol sebacate) as a nerve guide material. Biomaterials. 2005; 26:5454–5464. [PubMed: 15860202]
24. Fidkowski C, Kaazempur-Mofrad MR, Borenstein J, Vacanti JP, Langer R, Wang YD. Endothelialized microvasculature based on a biodegradable elastomer. Tissue Eng. 2005; 11:302–309. [PubMed: 15738683]
25. Engelmayr GC Jr, Cheng M, Bettinger CJ, Borenstein JT, Langer R, Freed LE. Accordion-like honeycombs for tissue engineering of cardiac anisotropy. Nat Mater. 2008; 7:1003–1010. [PubMed: 18978786]
26. Kenar H, Kose GT, Toner M, Kaplan DL, Hasirci V. A 3D aligned microfibrous myocardial tissue construct cultured under transient perfusion. Biomaterials. 2011; 32:5320–5329. [PubMed: 21570112]
27. Ravichandran R, Venugopal JR, Sundarrajan S, Mukherjee S, Sridhar R, Ramakrishna S. Minimally invasive injectable short nanofibers of poly(glycerol sebacate) for cardiac tissue engineering. Nanotechnology. 2012:23.

28. Ravichandran R, Venugopal JR, Sundarrajan S, Mukherjee S, Ramakrishna S. Poly(glycerol sebacate)/gelatin core/shell fibrous structure for regeneration of myocardial infarction. Tissue Eng Part A. 2011; 17:1363–1373. [PubMed: 21247338]
29. Masoumi N, Jean A, Zugates JT, Johnson KL, Engelmayr GC Jr. Laser microfabricated poly(glycerol sebacate) scaffolds for heart valve tissue engineering. J Biomed Mater Res A. 2013; 101A:104–114. [PubMed: 22826211]
30. Shin SR, Jung SM, Zalabany M, Kim K, Zorlutuna P, Kim SB, et al. Carbon-nanotube-embedded hydrogel sheets for engineering cardiac constructs and bioactuators. ACS Nano. 2013 In Press.
31. Ng CP, Hinz B, Swartz MA. Interstitial fluid flow induces myofibroblast differentiation and collagen alignment in vitro. J Cell Sci. 2005; 118:4731–4739. [PubMed: 16188933]
32. Kim SB, Bae H, Cha JM, Moon SJ, Dokmeci MR, Cropek DM, et al. A cell-based biosensor for real-time detection of cardiotoxicity using lensfree imaging. Lab Chip. 2011; 11:1801–1807. [PubMed: 21483937]
33. Pelouch V, Dixon IMC, Golfman L, Beamish RE, Dhalla NS. Role of extracellular-matrix proteins in heart function. Mol Cell Biochem. 1993; 129:101–120. [PubMed: 8177233]
34. Mwangi JW, Ofner CM. Crosslinked gelatin matrices: release of a random coil macromolecular solute. Int J Pharm. 2004; 278:319–327. [PubMed: 15196637]
35. Sun Z-J, Wu L, Huang W, Zhang X-L, Lu X-L, Zheng Y-F, et al. The influence of lactic on the properties of Poly (glycerol-sebacate-lactic acid). Mater Sci Eng C Mater Biol Appl. 2009; 29:178–182.
36. Liang S-L, Yang X-Y, Fang X-Y, Cook WD, Thouas GA, Chen Q-Z. In Vitro enzymatic degradation of poly (glycerol sebacate)-based materials. Biomaterials. 2011; 32:8486–8496. [PubMed: 21855132]
37. Jacot JG, McCulloch AD, Omens JH. Substrate stiffness affects the functional maturation of neonatal rat ventricular myocytes. Biophys J. 2008; 95:3479–3487. [PubMed: 18586852]
38. McDonald KS, Wolff MR, Moss RL. Force-velocity and power-load curves in rat skinned cardiac myocytes. J Physiol. 1998; 511:519–531. [PubMed: 9706028]
39. Zhang YZ, Venugopal J, Huang ZM, Lim CT, Ramakrishna S. Crosslinking of the electrospun gelatin nanofibers. Polymer. 2006; 47:2911–2917.
40. Li MY, Guo Y, Wei Y, MacDiarmid AG, Lelkes PI. Electrospinning polyaniline-contained gelatin nanofibers for tissue engineering applications. Biomaterials. 2006; 27:2705–2715. [PubMed: 16352335]
41. Baji A, Mai Y-W, Wong S-C, Abtahi M, Chen P. Electrospinning of polymer nanofibers: effects on oriented morphology, structures and tensile properties. Compos Sci Technol. 2010; 70:703–718.
42. Lu J-W, Zhang Z-P, Ren X-Z, Chen Y-Z, Yu J, Guo Z-X. High-elongation fiber mats by electrospinning of polyoxymethylene. Macromolecules. 2008; 41:3762–3764.
43. Wu X-F, Dzenis YA. Size effect in polymer nanofibers under tension. J Appl Phys. 2007:102.
44. Discher DE, Janmey P, Wang YL. Tissue cells feel and respond to the stiffness of their substrate. Science. 2005; 310:1139–1143. [PubMed: 16293750]
45. Woo KM, Chen VJ, Ma PX. Nano-fibrous scaffolding architecture selectively enhances protein adsorption contributing to cell attachment. J Biomed Mater Res A. 2003; 67A:531–537. [PubMed: 14566795]
46. Jose MV, Thomas V, Dean DR, Nyairo E. Fabrication and characterization of aligned nanofibrous PLGA/collagen blends as bone tissue scaffolds. Polymer. 2009; 50:3778–3785.
47. Lee J, Tae G, Kim YH, Park IS, Kim S-H, Kim SH. The effect of gelatin incorporation into electrospun poly(L-lactide-co-epsilon-caprolactone) fibers on mechanical properties and cytocompatibility. Biomaterials. 2008; 29:1872–1879. [PubMed: 18234330]
48. Kwon IK, Matsuda T. Co-electrospun nanofiber fabrics of poly(L-lactide-co-epsilon-caprolactone) with type I collagen or heparin. Biomacromolecules. 2005; 6:2096–2105. [PubMed: 16004450]
49. Lijnen P, Petrov V. Renin-angiotensin system, hypertrophy and gene expression in cardiac myocytes. J Mol Cell Cardiol. 1999; 31:949–970. [PubMed: 10336836]

50. Poobalarahi F, Baicu CF, Bradshaw AD. Cardiac myofibroblasts differentiated in 3D culture exhibit distinct changes in collagen I production, processing, and matrix deposition. Am J Physiol Heart Circ Physiol. 2006; 291:H2924–H2932. [PubMed: 16891407]
51. Gabbiani G. The myofibroblast in wound healing and fibrocontractive diseases. J Pathol. 2003; 200:500–503. [PubMed: 12845617]
52. Eguchi S, Dempsey PJ, Frank GD, Motley ED, Inagami T. Activation of MAPKs by angiotensin II in vascular smooth muscle cells - Metalloprotease-dependent EGF receptor activation is required for activation of ERK and p38 MAPK but not for JNK. J Biol Chem. 2001; 276:7957–7962. [PubMed: 11116149]
53. Schorb W, Booz GW, Dostal DE, Conrad KM, Chang KC, Baker KM. Angiotensinii is mitogenic in neonatal rat cardiac fibroblasts. Circ Res. 1993; 72:1245–1254. [PubMed: 8495553]
54. Wang J, Seth A, McCulloch CAG. Force regulates smooth muscle actin in cardiac fibroblasts. Am J Physiol Heart Circ Physiol. 2000; 279:H2776–H2785. [PubMed: 11087232]
55. Wang J, Chen H, Seth A, McCulloch CA. Mechanical force regulation of myofibroblast differentiation in cardiac fibroblasts. Am J Physiol Heart Circ Physiol. 2003; 285:H1871–H1881. [PubMed: 12842814]
56. Castella LF, Buscemi L, Godbout C, Meister J-J, Hinz B. A new lock-step mechanism of matrix remodelling based on subcellular contractile events. J Cell Sci. 2010; 123:1751–1760. [PubMed: 20427321]
57. Boateng SY, Hartman TJ, Ahluwalia N, Vidula H, Desai TA, Russell B. Inhibition of fibroblast proliferation in cardiac myocyte cultures by surface microtopography. Am J Physiol Cell Physiol. 2003; 285:C171–C182. [PubMed: 12672651]
58. Grinnell F, Ho CH, Tamariz E, Lee DJ, Skuta G. Dendritic fibroblasts in three-dimensional collagen matrices. Mol Biol Cell. 2003; 14:384–395. [PubMed: 12589041]
59. Nikkhah M, Eshak N, Zorlutuna P, Annabi N, Castello M, Kim K, et al. Directed endothelial cell morphogenesis in micropatterned gelatin methacrylate hydrogels. Biomaterials. 2012; 33:9009–9018. [PubMed: 23018132]
60. Parrag IC, Zandstra PW, Woodhouse KA. Fiber alignment and coculture with fibroblasts improves the differentiated phenotype of murine embryonic stem cell-derived cardiomyocytes for cardiac tissue engineering. Biotechnol Bioeng. 2012; 109:813–822. [PubMed: 22006660]
61. Wu KH, Mo XM, Liu YL, Zhang YS, Han ZC. Stem cells for tissue engineering of myocardial constructs. Ageing Res Rev. 2007; 6:289–301. [PubMed: 17981518]
62. Schulz R, Heusch G. Connexin 43 and ischemic preconditioning. Cardiovasc Res. 2004; 62:335–344. [PubMed: 15094353]

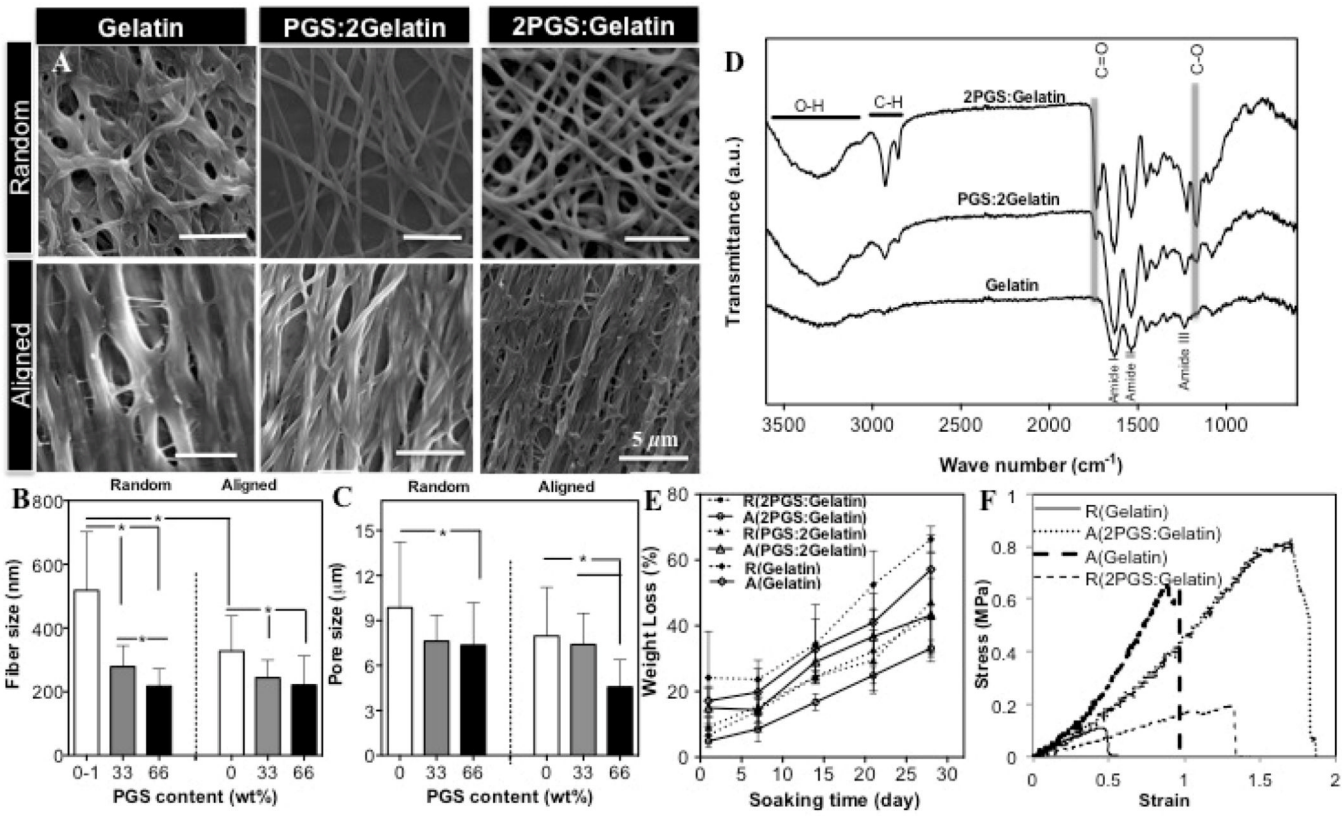

Figure 1.

Structural properties of crosslinked PGS:gelatin scaffolds; (A) SEM images of crosslinked fibrous scaffolds. (B) Fiber size, (C) Pore sizes, and (D) FTIR spectra of crosslinked fibrous scaffolds. (E) Representative degradation curves of scaffolds following soaking in DPBS. (F) Representative uniaxial tensile stress-strain plots of crosslinked aligned (in the preferred direction) and random Gelatin and 2PGS:Gelatin scaffolds after 2 days soaking in culture medium (*: $P<0.05$).

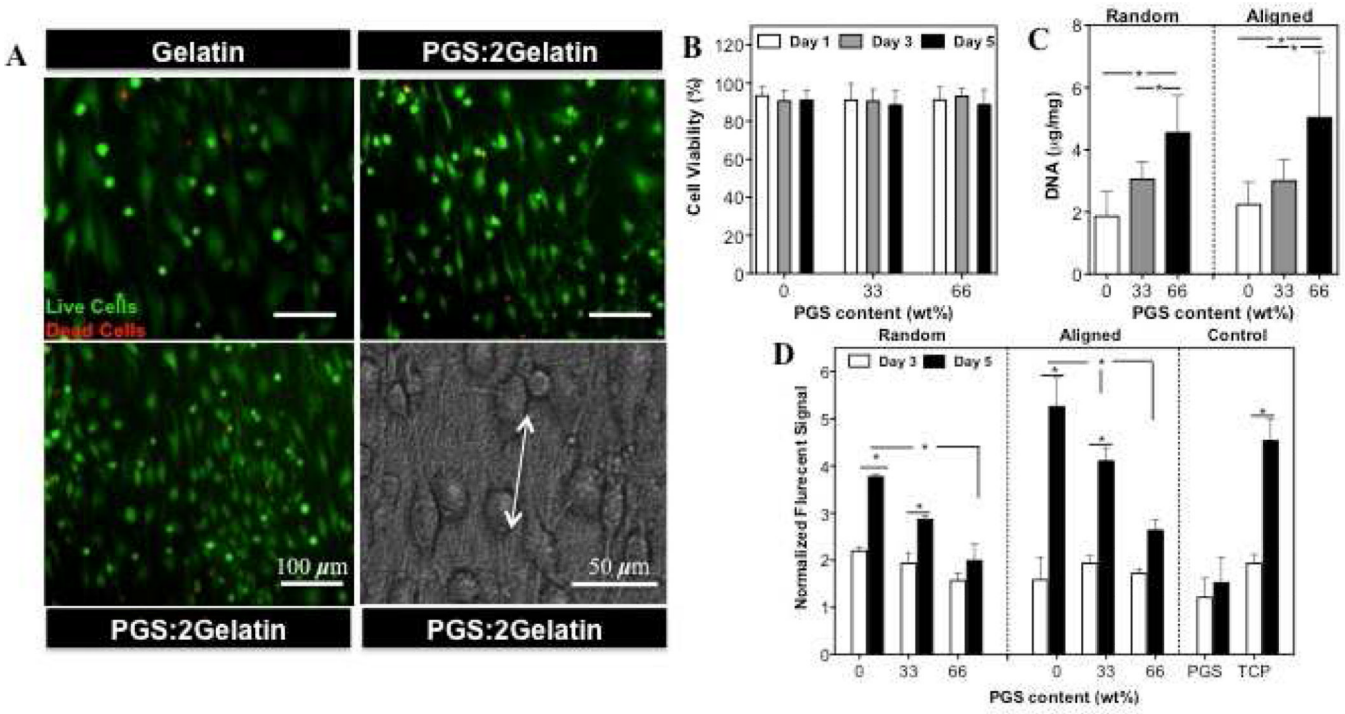

Figure 2.

(A) Representative images of live/dead assay and phase contrast images of CFs seeded on the aligned scaffolds at day 1 of culture (Live cells: green stain, Dead cells: red stain). (B) Quantified viability results obtained at days 1, 3 and 5 of culture. (C) DNA quantification of CFs cultured for 6h on the aligned and random scaffolds. (D) Normalized CFs metabolic activity determined by Alamar Blue assay at days 3 and 5 of culture. (*: $P<0.05$).

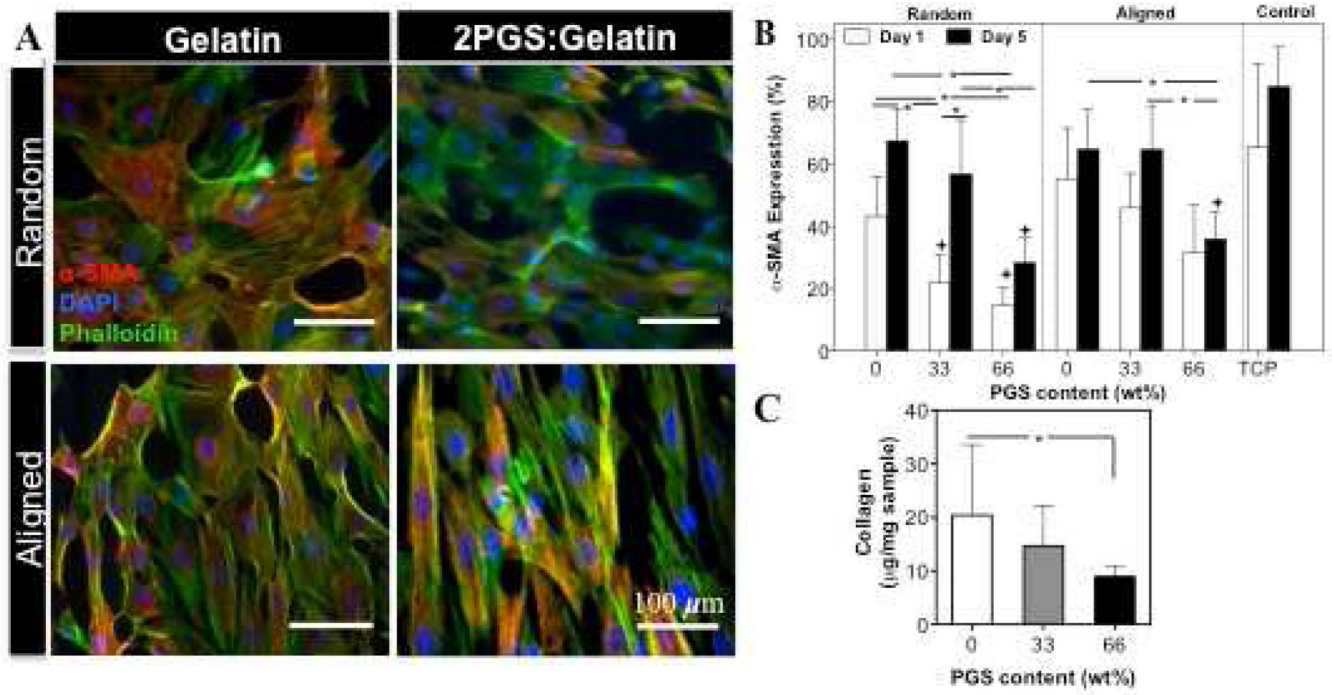

Figure 3.

(A) Effects of physical and chemical properties of scaffolds on the on differentiation of CFs. Low PGS content along with fiber alignment increased the number of α-SMA–positive CFs. Overlaid images of CFs cultured for 5 days on random and aligned scaffolds stained for α-SMA (red), F-actin (green) and DAPI (blue). (B) Quantification of α-SMA expressing cells cultured on the aligned and random scaffolds on days 1 and 5 of culture. (C) SirCol™ assay analysis, confirming that the amount of the deposited collagen per sample significantly increased on A(Gelatin) scaffold after 5 days of culture.(+ and *:Compared to control and other scaffolds, respectively.(*and +: $P<0.05$)).

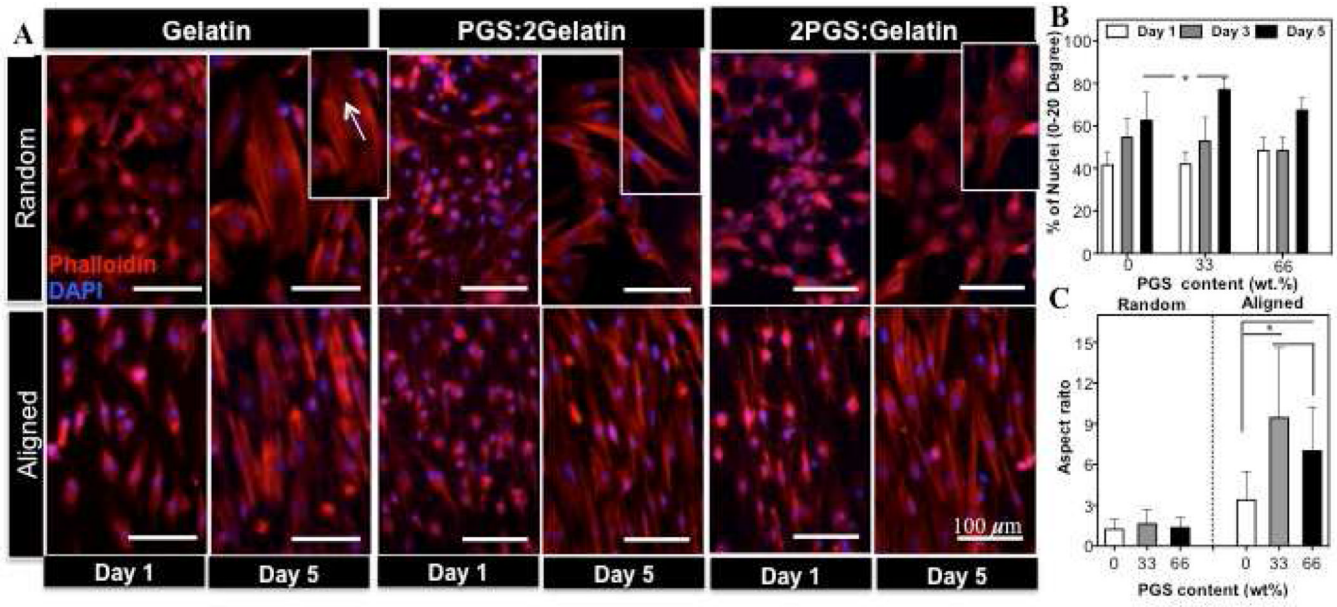

Figure 4.

Effects of scaffold compositions and architecture on the morphology, alignment and elongation of CFs. (A) Actin filaments and nuclei stained CFs with Phalloidin and DAPI on the random and aligned scaffolds. Main panels indicate the orientation and morphology of cells. Insets: higher magnification images showing elongated stress fibers within the cells cytoplasm increasing with lower PGS content. Quantified (B) alignment and (C) elongation of CFs on each scaffold. Cell alignment was significantly higher on A(PGS:2Gelatin) scaffold compared to A(Gelatin) scaffold (*: $P < 0.05$).

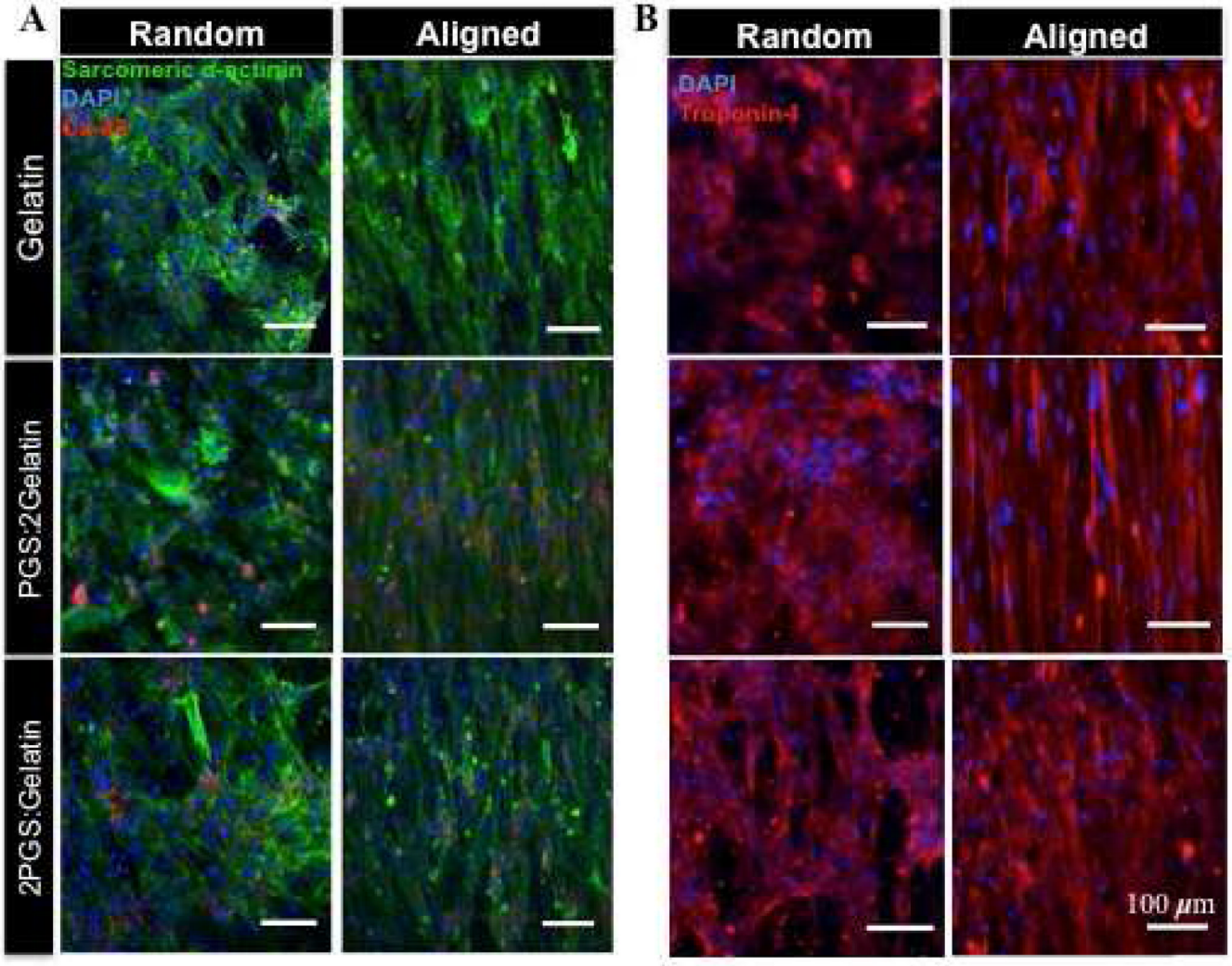

Figure 5.
Representative fluorescence images of CMs immunostained for (A) Sarcomeric α-actinin (green), Cx-43 (red) and DAPI (blue), and (B) cardiac troponin I (red) on the aligned and random scaffolds.

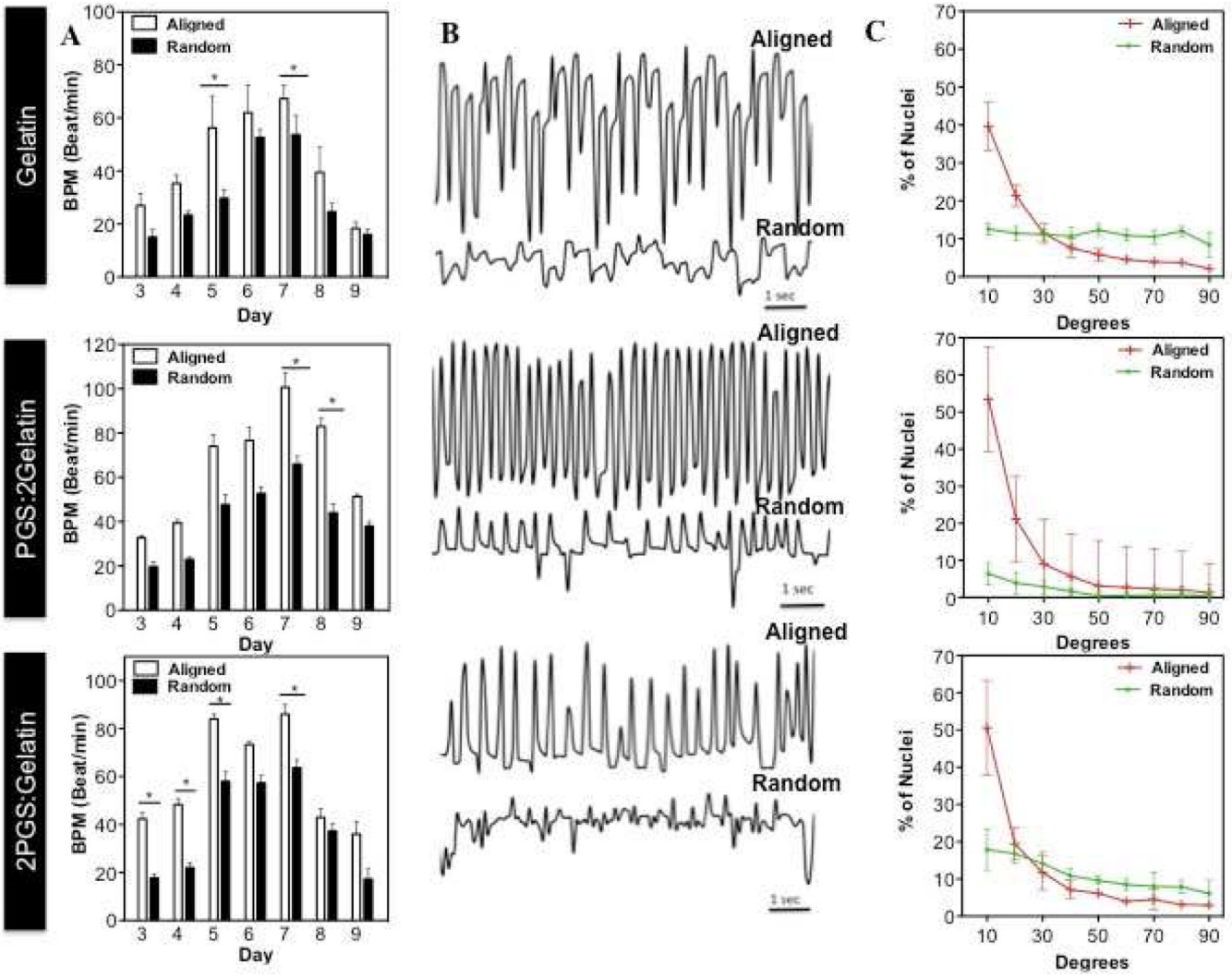

Figure 6.

Interactive effects of physical and chemical properties on CMs contraction and organization. (A) Beating rates (BPM) and (B) beating patterns of the CMs cultured on the aligned and random scaffolds at different culture periods. Cell beating frequency was recorded at day 7 of culture. (C) CMs alignment was quantified after 7 days of culture. (*: $P < 0.05$)

Table 1

Mechanical properties of crosslinked aligned (A) and random (R) scaffolds at dry and wet (after 2 days in culture medium) states.

Sample	Tensile Strength (MPa)		Tensile Modulus (MPa)		Elongation(%)	
	Dry	Wet	Dry	Wet	Dry	Wet
A(2PG5:Gelatin)	1.63±0.2	1.07±0.6	20.10±3.5*	0.36±0.1*	21.4±10**	229±103*
R(2PG5:Gelatin)	1.49±0.1*	0.28±0.3*	9.31±1.3*	0.14±0.1	31.2±10*	182±152*
A(PGS:2Gelatin)	1.98±.3	0.89±0.2	43.96±5.4	0.59±0.2	15.1±4	119±28
R(PGS:2Gelatin)	1.62±1.4*	0.32±0.2	13.69±4.8	0.29±0.2	337±22	93±11*
A(Gelatin)	3.91±2.8	0.88±0.3	82.29±21.3	0.72±0.1	6.4±2	108±38
R(Gelatin)	2.22±1.7	0.48±0.3	54.36±19.7	0.35±0.2	14.6±10	93±54

** and *** Compared to R(Gelatin) and A(Gelatin) fibrous scaffold, respectively ($P<0.05$)